

Electric polarization and dynamics of molecular motion of polar liquid crystals in micropores and macropores

F. M. Aliev and M. N. Breganov

Institute of Precision Mechanics and Optics, Leningrad

(Submitted 7 June 1987)

Zh. Eksp. Teor. Fiz. **95**, 122–138 (January 1989)

Dielectric spectroscopy was used in an investigation of equilibrium and kinetic properties of polar liquid crystals in micropores (with a pore radius up to 65 Å) and macropores (1000 Å) in silicate matrices. The thickness of a layer with polar ordering ($l \approx 100$ Å), the total surface energy of the interaction between molecules and the substrates ($F_0 \approx 10^2$ erg/cm²), and the anisotropic part of this energy ($W \approx 1$ erg/cm²) representing the energy of adhesion of a nematic liquid crystal to the pore wall are calculated. A soft mode exhibiting critical slowing down (relaxation time τ), absent in the case of a nematic liquid crystal in the free state, was observed for the first time in micropores. The critical exponent of the dependence $\tau(T_c - T)$ was found to be unity.

1. INTRODUCTION

Physical properties of liquids and solids in small pores are attracting major attention of theoreticians and experimentalists. This is due to the fact that these properties can provide clear information on the surface and size effects in the condensed state of matter.

Characteristics of physical properties of pores in various sizes and shapes have already been investigated for ³He and ⁴He (Refs. 1–3), while ³He is the only material for which not only equilibrium but also relaxation properties have been studied. The influence of the pore surface gives rise to surface relaxation processes in solid and liquid phases of ³He (Refs. 2 and 3) of the kind absent in the free state.

The differences between the surface and bulk properties as well as the size effects are manifested most strikingly in the case of nematic liquid crystals. This is due to the fact that such liquid crystals are "soft" systems because the energy responsible for the long-range orientational order is fairly small.⁴ It follows that the substrates between which a layer of a nematic liquid crystal is confined can exert their influence on the liquid crystal to distances L_0 which may reach several thousands of angstroms.^{4,5} It is clear from the above discussion that investigations of nematic liquid crystals in pores of size less than L_0 should, in principle, provide information on the surface properties of these liquid crystals. It is at distances of the order of L_0 from the surface of the substrate that the equilibrium properties of nematic liquid crystals (for example, the order parameter⁵) differ from the bulk properties. However, the influence of the substrate on the orientational mobility of liquid crystal molecules and the distance at which such an influence is still manifested have not yet been investigated.

There is a fundamental problem, which is also of practical importance, of the energy W of adhesion of a liquid crystal to a solid substrate. An estimate of W obtained on the basis of general physical principles⁴ gives 10 erg/cm², whereas the experimental values of W range from 10^{-5} erg/cm² to 1 erg/cm² (see, for example, Refs. 4 and 6 and the literature cited there). There are also doubts about the shift of the temperature of the phase transition of a nematic liquid crystal to an isotropic phase inside a pore or in a thin film. The question arises whether this temperature is higher^{7–9} or lower^{10–12} than the corresponding bulk value and whether the shift of the transition temperature is a pure size effect or

is affected by the energy of the interaction between the molecules and the substrate. Finally, in the case of polar liquid-crystal molecules the substrate surface may induce a polar order and give rise to the associated surface polarization effects^{13,14} which can also be due to a gradient of the order parameter and inhomogeneity of the orientation.¹⁵ Clearly, the bent nature of the pore surface may induce these effects in porous matrices.

All these aspects of the surface properties of liquid crystals are basically problematic or at best there is some doubt about them.

We investigated these topics by the method of dielectric spectroscopy which in a single experiment provides information on the orientational mobility of molecules, formation of the structure, and phase transitions. We investigated strongly polar liquid crystals, characterized by different values of the angle β between the dipole and the long axis of a molecule, which were introduced into micropores and macropores in silicate matrices.

2. SAMPLES AND MEASUREMENT METHOD

We investigated the following liquid crystals.

1) Pentylcyanobiphenyl (5CB) with the temperatures of the transitions to the nematic and isotropic phases $T_{CN} = 295$ K and $T_{NI} = 308$ K, respectively. The dipole moment μ of the 5CB molecule is 5 D and it is parallel to the longitudinal axis of the molecule ($\beta = 0$). Equilibrium and relaxation dielectric properties of 5CB, like those of other alkylcyanobiphenyls have been investigated thoroughly.¹⁶ In the free state the dispersion of the principal values of the permittivity of the nematic phase of 5CB is related to rotation of the molecules about the short axis and precession of the long axis around the direction of the vector, whereas the mode associated with the rotation of the molecule about the long axis is not observed because the dipole moment of the molecule is directed along this axis.

2) Two related liquid crystals 4*n*-hexoxy-4'-*n*-pentyl- α -cyanostilbene (ACS-1) with $T_{CN} = 302$ K, $T_{NI} = 321.5$ K, $\mu = 3.8$ D, and $\beta = 64^\circ$ differs in respect of the transition temperatures $T_{CN} = 309$ K and $T_{NI} = 320.2$ K from 4*n*-pentyl-4-*n*-hexoxy- α -cyanostilbene (ACS-2). The results of dielectric investigations of ACS-1 are reported in Ref. 17. Unusual relaxation phenomena in ACS due to the absence of dispersion of the permittivity along the director at frequen-

cies in the range 10^3 – 10^6 Hz have been reported also for four similar α -cyanostilbenes.¹⁸

3) Cyanophenyl ester of heptylbenzoic acid, i.e., cyanophenyl heptylbenzoate (CPHB) has the transition temperatures $T_{CN} = 316.5$ K and $T_{NI} = 328.1$ K. The molecules of this substance have a record-high (for liquid crystals) dipole moment: $\mu = 6.1$ D, $\beta = 16^\circ$.

All the investigated liquid crystals were synthesized at the Vilnius State University and kindly supplied to us by P. V. Adomenas.

Porous matrices with through pores were prepared from the original sodium borosilicate glasses by a method described in Ref. 19: the sodium borate phase was removed by leaching and the matrix framework consisted of SiO_2 . We used two types of matrices with the properties (pore radius R , volume fraction of the phases ω , and specific surface area S/V) determined by the method of low-angle x-ray scattering²⁰: $R_1 = 65$ Å, $\omega_1 = 0.27$, $(S/V)_1 = 100$ m² per cm³ in the case of microporous matrices and $R_2 = 1000$ Å, $\omega_2 = 0.38$, and $(S/V)_2 = 28$ m² per cm³ in the case of macroporous matrices.

Our samples were porous glass plates, of $2 \times 2 \times 0.1$ cm dimensions, heated to 150°C and pumped out; this was followed by impregnation with the investigated liquid crystals from an isotropic melt. Measurements of the real part ϵ' of the complex permittivity were made using an external electric field of frequency ν ranging from 10^3 Hz to 7×10^7 Hz, whereas the imaginary part ϵ'' was determined at frequencies from 5×10^5 Hz to 7×10^7 Hz employing apparatus used earlier^{17,18} in a study of liquid crystals in the free state, which was supplemented by a semiautomatic impedance and transmission meter of the Tesla-BM538 type, which was calibrated between 0.5 and 70 MHz. A parallel-plate titanium capacitor was used as a measuring cell: two investigated plates were located between one inner and two outer ground electrodes. The relative error in the determination of ϵ' did not exceed 1% in the range of $\nu < 1.5 \times 10^6$ Hz and not more than 3% at higher frequencies; the dielectric losses were determined to within 10%. The temperature of the cell was stabilized and measured to within $\pm 0.1^\circ\text{C}$. The permittivities of empty porous matrices were $\epsilon_1 = 3.9$ (microporous samples) and $\epsilon_2 = 3.5$ (macroporous samples); in the investigated ranges of the temperature T and frequency ν these permittivities were independent of T and ν . The permittivities ϵ_f of the framework material in microporous and macroporous matrices, determined for sintered samples after leaching out the sodium borate phase, were found—as expected—to be identical and equal to $\epsilon_f = 4.82$; they were independent of the frequency and temperature. This observation and the practically negligible electrical conductivity of the matrices (disperse phase) simplified the interpretation of the results and avoided a number of difficulties that have been encountered earlier in studies of dielectric properties of heterogeneous systems.²¹

The quantities measured directly were the permittivities ϵ'_c and the dielectric loss factors ϵ''_c two-phase heterogeneous systems comprising a matrix and a nematic liquid crystal. The permittivity ϵ_{lc} of the disperse phase (liquid crystal) calls for a theory allowing for the anisotropy and local inhomogeneity of a nematic liquid crystal dispersed in a matrix and valid at high concentrations of the liquid crystal. Such a theory is not known to the present authors so that

we had to calculate the permittivity of the second phase (liquid crystal) using the following relationship²¹ valid in the case of isotropic spherical inclusions:

$$\epsilon'_c = \epsilon'_f + (\epsilon'_{lc} - \epsilon'_f)f\omega, \quad (1)$$

where $f = (\epsilon'_c + 2\epsilon'_f)/3\epsilon'_f$ and ω is the volume fraction of the nematic liquid crystal. Application of Eq. (1) to empty matrices, bearing in mind that in this case the permittivity of the second phase (voids) is unity and using $\omega_1 = 0.27$ and $\omega_2 = 0.38$, yielded the value $\epsilon_f = 4.82$ for the microporous and macroporous matrices, as found by direct experiments.

The capacitance of a capacitor containing any of the investigated samples, measured in a magnetic field of 6 kG intensity sufficient to establish a uniform orientation in a free nematic liquid crystal, was always equal to the capacitance determined in the absence of a magnetic field. This was due to the fact that the distance L_0 , in which the static properties of a nematic liquid crystal, due to the orienting effect of the substrate, differed from the bulk values by at least $R_2 = 1000$ Å.

We shall use $\langle \epsilon \rangle$ to denote the volume-averaged real part of the permittivity of a given liquid crystal in the pores, calculated from Eq. (1). A satisfactory theory may first of all alter the absolute values of $\langle \epsilon \rangle$, but it should have less effect on the nature of the temperature and frequency dependences which are discussed below.

In the investigation of the frequency dependences of ϵ'_c of heterogeneous systems we must bear in mind that although one component of the system is conducting and has a high electrical conductivity σ , the separate components of the system can exhibit, even in the absence of dispersion of the permittivity, a dielectric dispersion which is due to the Maxwell-Wagner polarization mechanism.²¹ In the case of spherical inclusions in a nonconducting medium ($\sigma_f = 0$) the relaxation time governed by the Maxwell-Wagner dispersion is²¹

$$\tau = \epsilon_0 \frac{2\epsilon_f + \epsilon_{lc} + \omega(\epsilon_f - \epsilon_{lc})}{\sigma_{lc}(1 - \omega)}, \quad (2)$$

where $\epsilon_0 = 8.854 \times 10^{-12}$ F/m and σ is traditionally measured in units of $\Omega^{-1} \cdot \text{m}^{-1}$. All the quantities on the right-hand side of Eq. (2) are known: $\epsilon_f = 4.82$, $\epsilon_{lc} \approx 10$ – 15 , $\omega = 0.27$ (micropores) or $\omega = 0.38$ (macropores). The value of σ_{lc} for liquid crystals subjected to careful purification should not be more than $10^{-10} \Omega^{-1} \cdot \text{m}^{-1}$ and at worse it should be $\sigma_{lc} = 10^{-6} \Omega^{-1} \cdot \text{m}^{-1}$. These are the limits and the use of them gives values $\tau > 3 \times 10^{-4}$ s, i.e., in the case of the investigated samples the dispersion associated with the inhomogeneity and heterogeneity of the system and due to the Maxwell-Wagner polarization mechanism should be manifested at frequencies $\nu < 10^3$ Hz. This is the reason why the relaxation times obtained at frequencies $\nu > 10^4$ Hz should be regarded as the dipole properties of the investigated liquid crystals in porous matrices.

3. 5CB IN MICROPORES AND MACROPORES

1. *The $\epsilon = \epsilon(T)$ dependence.* The temperature dependence of $\langle \epsilon \rangle$ determined at a frequency of 1 kHz in micropores exhibits a clear hysteresis (curves 1 and 1' in Fig. 1). We also determined the temperature dependences of $\langle \epsilon \rangle$ for 5CB in macropores (curves 2 and 3). We found that there was a pronounced change in the permittivity at temperatures

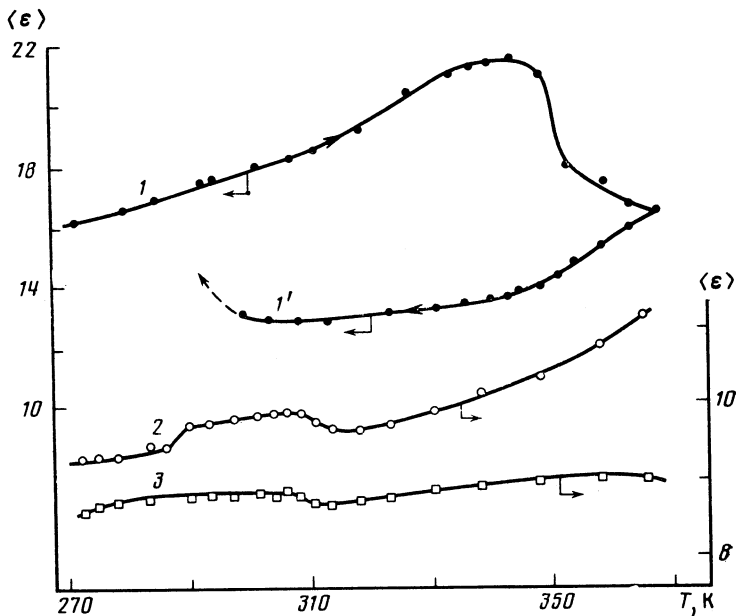


FIG. 1. Temperature dependences of the permittivity of 5CB: 1), 1') in micropores (1 kHz); 2), 3) in macropores (1 and 150 kHz, respectively).

347–351 K (curve 1). Similar singularities were exhibited also by curve 2: the first at $T \approx 310.5$ K and the second at $T \approx 298$ K. If the temperatures 348 K for curve 1 and 310.5 K for curve 2 are interpreted as the phase transition temperatures $T_{NI}^{(R)}$ from the nematic to the isotropic phase, we may draw the conclusion that the pores tend to create an orientational order and increase T_{NI} in pores compared with the corresponding value for 5CB in the free state. The second singularity (at $T_{CN}^{(R)} = 289$ K) observed on curve 2 is atypical, observed in dielectric measurements, feature of a transition from the solid to the nematic phase. In other words, as in all the cases discussed before, the melting point of the liquid phase in pores is lowered.¹⁰ A quantitative interpretation of the shift of the phase transition temperatures is given in Sec. 6.

Thermal hysteresis of ϵ observed for 5CB in micropores was accompanied also by an optical hysteresis when light transmission was plotted as a function of temperature (Fig. 2). Hence, the optical hysteresis observed earlier in a study of a cholesteric liquid crystal in micropores²² and all the characteristics of this effect are shared by other liquid crystals. The temperature at which our sample became completely transparent ($T = 347.5$ K) could be regarded as $T_{NI}^{(R)}$ in the pores and it is close to the corresponding temperature in the case of curve 1 in Fig. 1.

As in the case of a cholesteric filling micropores,²² a strong turbidity (with a transmission coefficient $A < 15\%$), observed at temperatures $T < 310$ K in the system with 5CB in a microporous matrix, could not be explained by an optical inhomogeneity (due to the difference between the refractive indices of the matrix material and of 5CB) or by molecular scattering of light. This turbidity could be due to the formation of fractal clusters as a result of cooling, which is a macroscopic effect and should be accompanied by strong scattering of light on the fractal structure.

2. The $\epsilon = \epsilon(\nu)$ dependence. It is clear from Fig. 3 (curves 1 and 2) that the dependences $\langle \epsilon(\nu) \rangle$ obtained for 5CB in micropores and macropores were clearly of relaxational nature and exhibited three regions of the permittivity dispersion. Figure 4 shows the results of measurements of

the frequency dependences ϵ'_c (curves 1' and 2') and, for the second region of dispersion, of ϵ''_c (curves 1a and 2a) observed at various temperatures for 5CB in a macroporous matrix and the permittivities $\langle \epsilon \rangle$ (curves 1 and 2) of this liquid crystal deduced from curves 1' and 2' using Eq. (1). Clearly, the points of inflection of curves 1 and 2 coincide with the positions of the maxima of the dependences $\epsilon''_c(\nu)$. The Cole-Cole diagrams $\epsilon''(\epsilon')$ are plotted (Fig. 5, curves 1 and 2) and they corresponded to the $\epsilon'_c(\nu)$ and $\epsilon''_c(\nu)$ dependences in Fig. 4. The Cole-Cole diagrams indicate that the parameters α , representing empirically the spectrum of the relaxation times, are $\alpha = 0.21$ at $T = 293$ K and $\alpha = 0.3$ at $T = 301$ K.

Plotting of the $\epsilon''(\epsilon')$ enabled us to separate the dispersion regions and to determine the values of the permittivities which in the second dispersion region were static and at the same time corresponded to the "high-frequency" plateau for

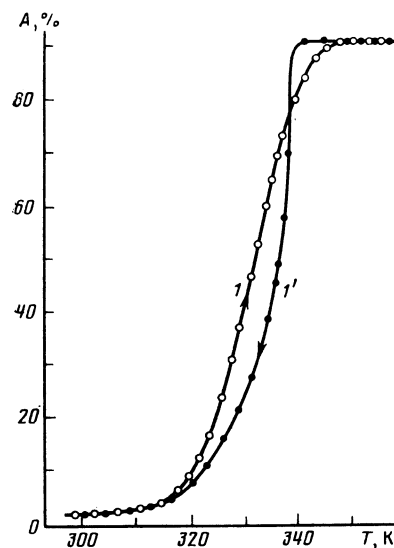


FIG. 2. Temperature dependences of the optical transmission coefficient A of 5CB in micropores: 1) during heating; 1') during cooling. Wavelength $\lambda = 5600$ Å.

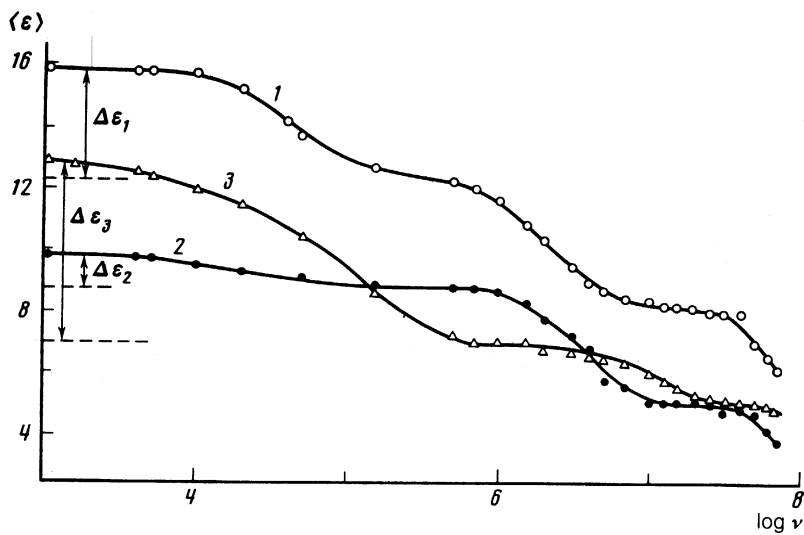


FIG. 3. Frequency dependences of the permittivity at $T = 290\text{ K}$: 1) 5CB in micropores; 2) 5CB in macropores; 3) CPHB in micropores. The dashed horizontal lines are the values of ϵ , for the second dispersion region.

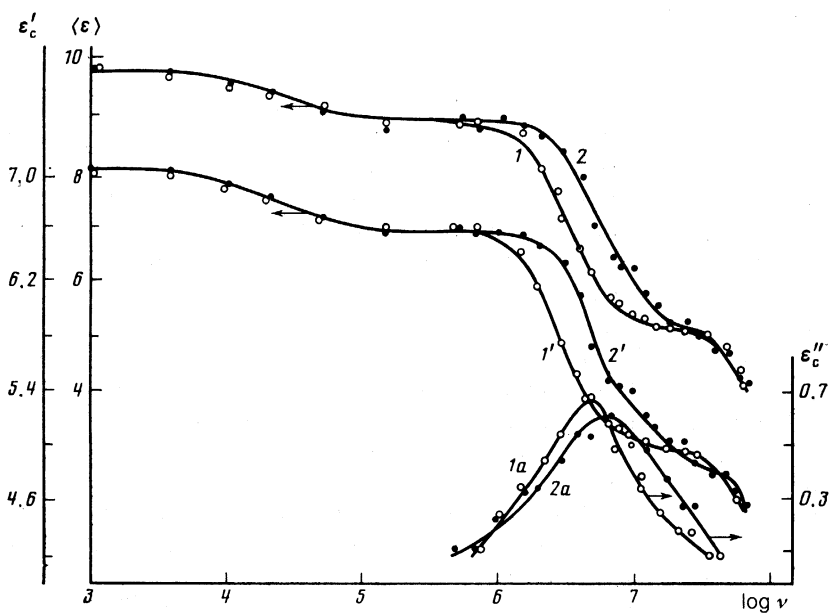


FIG. 4. Frequency dependences of the permittivity and the dielectric loss factors of 5CB in macropores: 1), 2) $\langle \epsilon \rangle$ at 298 and 301 K (respectively); 1'), 2') ϵ''_c ; 1a), 2a) ϵ''_c .

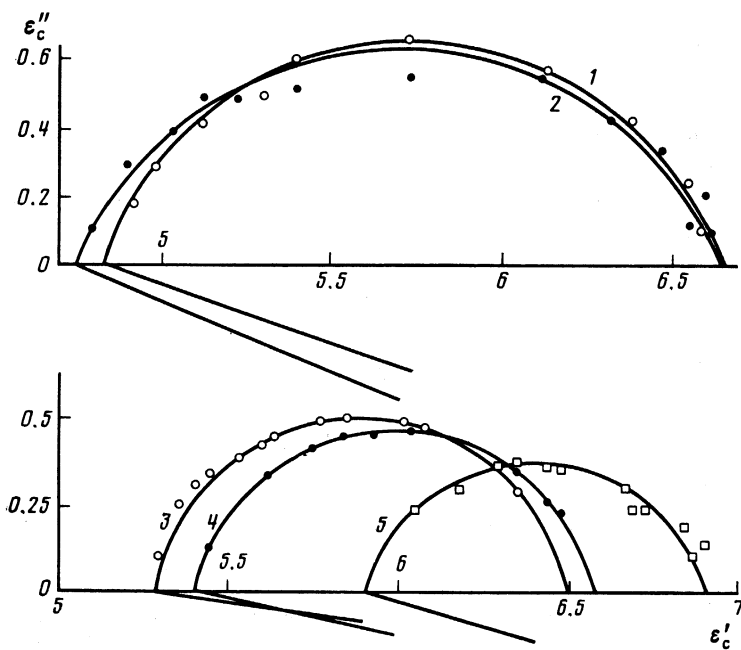


FIG. 5. Cole-Cole diagrams: 1), 2) 5CB in macropores at 293 and 301 K, respectively; 3), 4), 5) CPHB in micropores at 318.5, 343, and 383 K, respectively.

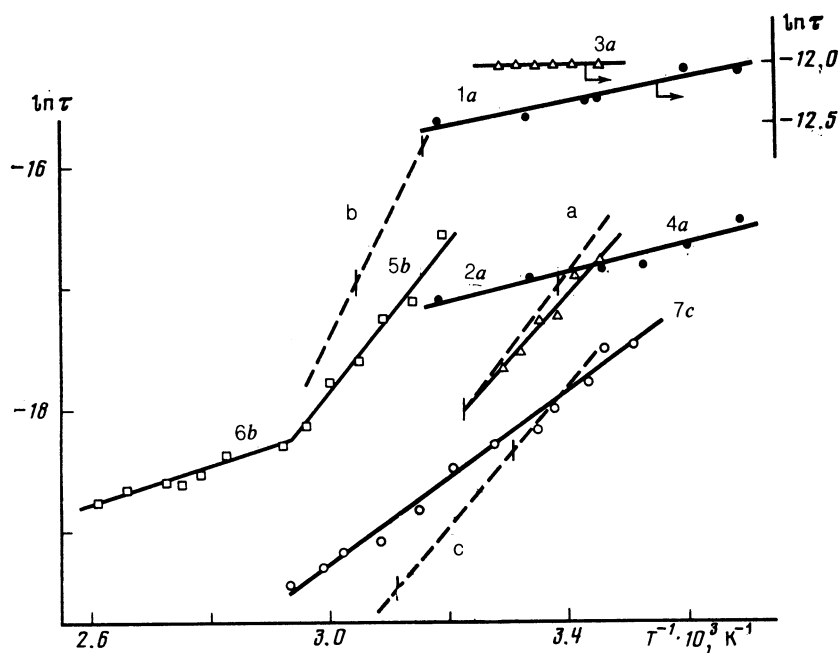


FIG. 6. Dependence of the dielectric relaxation on the reciprocal temperature: a) 5CB; b) CPHB; c) ACS-1 in the free state. Vertical segments define the range of existence of the nematic phase. Relaxation time: 1a) τ_1 ; 2a) τ_2 , (both obtained for 5CB in micropores); 3a) τ_1 , 4a) τ_2 (5CB in macropores); 5b), 6b), τ_2 (CPHB in micropores); 7c) τ_2 (ACS-1 in micropores).

the first dispersion region. These values, calculated from Eq. (1), are identified by dashed curves in Fig. 3. This procedure was applied to all the investigated samples; this made it possible to determine the relaxation times describing the first and second dispersion regions from the Debye equation modified by Cole and Cole:

$$\varepsilon'(\nu) = \varepsilon'_{2hf} + \frac{\varepsilon'_{1s} - \varepsilon'_{1hf}}{1 + 4\pi^2\nu^2\tau_1^2} + \frac{\varepsilon'_{2s} - \varepsilon'_{2hf}}{(1 + 4\pi^2\nu^2\tau_2^2)^{1-\alpha_2}}, \quad (3)$$

where ε'_{1s} and ε'_{2s} are the quasistatic values of ε' for the first and second dispersion regions; ε'_{1hf} and ε'_{2hf} are the corresponding "high-frequency" plateaus ($\varepsilon'_{1hf} = \varepsilon'_{2s}$); τ_1 and τ_2 are the relaxation times; α_2 is the Cole-Cole parameter for the second dispersion region; α_1 is assumed to be zero.

The relaxation times τ_1 and τ_2 were determined by fitting the calculated $\varepsilon'(\nu)$ dependences to the experimental results by the least-squares method. An analysis of the results employing a DVK-3M personal computer made it possible to include large amounts of experimental data in the calculations and to fit the experimental and calculated curves within the limits set by the experimental error. Clearly, the relaxation times found in this way for the second dispersion region were identical with those determined directly from measurements of $\varepsilon''(\nu)$ and this made it possible to plot the $\varepsilon''(\varepsilon')$ dependence.

The relaxation times found using Eq. (3) for the first two dispersion regions are plotted in Fig. 6 as a function of the reciprocal of temperature. The dashed lines in Fig. 6 represent the relaxation times τ_{\parallel} for 5CB and CPHB, as well as τ_1 for ACS-1, corresponding to the rotation of the molecules around the short (τ_{\parallel}) and long (τ_{\perp}) axes.

In the third dispersion region we were able to find only the order of magnitude of the relaxation time τ_3 , on the assumption that $\varepsilon_{\infty} = 2.3$, since in the case of 5CB in the free state the corresponding relaxation time was $\tau_3 \sim 5 \times 10^{-9}$ s, which was close to τ corresponding to a precession mechanism of dispersion of a free nematic liquid crystal.

3. Characteristics of the polarization and relaxation, and the thickness of a layer with polar ordering. The main differ-

ence between the behavior of the permittivity of 5CB in pores and the behavior in the free state was the existence of a low-frequency dispersion region, absent in the case of 5CB in the free state and characterized by relaxation times $\tau_1 \sim 10^{-6}$ s, which could not be attributed to the orientational motion of the molecules, but represented a collective process. The value of τ_1 for micropores depended weakly on temperature and in the case of macropores there was no temperature dependence of τ_1 .

The relaxation time τ_0 for the second region was close to τ_{\parallel} for the free state, but the temperature dependence of τ_2 was weaker both in micropores and macropores. The values of τ_2 and their temperature dependences in macropores were closer to the bulk behavior than the behavior observed in micropores, in agreement with expectations.

All these properties and the thermal hysteresis in micropores can be explained by postulating the appearance of a smectic order next to the wall of a pore.⁴ In fact, it is known that the $\varepsilon'(T)$ dependence for free liquid crystals in the smectic *A* and *C* phases exhibits a hysteresis²³ and the temperature dependence of the relaxation times governing the rotational mobility of molecules around the short axis becomes weaker²⁴ than in the nematic phase.

The Cole-Cole parameter for the free state of the nematic phase 5CB is $\alpha = 0$. Inside the pores we have $\alpha_2 \neq 0$ and there is then a spectrum of relaxation times. This is due to the fact that the properties of the surface layers begin to vary at distances of the order of molecular dimensions and, depending on the distance from the surface of a pore, the various layers of a liquid crystal can have different relaxation times.

The main argument in support of the existence of polar ordering at the wall is the low-frequency dispersion. It is natural to assume that the ratio of the low-frequency increments $\Delta\varepsilon_2$ and $\Delta\varepsilon_1$ corresponding to curves 2 and 1 in Fig. 3 is proportional to the volume fraction g of the surface layer of thickness l with polar ordering and located in macropores, if all the molecules in micropores belong to this layer. Then, if a macropore is modeled by a sphere or a cylinder of radius R_2 , we find that

$$\Delta\epsilon_2/\Delta\epsilon_1 \approx g = 1 - (R_2 - l)^3/R_2^3 \quad (\text{sphere}), \quad (4a)$$

$$\Delta\epsilon_2/\Delta\epsilon_1 \approx g = 1 - (R_2 - l)^2/R_2^2 \quad (\text{cylinder}). \quad (4b)$$

Using the experimental values $\Delta\epsilon_1 = 3.5$ and $\Delta\epsilon_2 = 1$ determined at the same temperature and assuming that $R_2 = 1000 \text{ \AA}$, we find from Eq. (4a) that $l = 110 \text{ \AA}$, whereas Eq. (4b) yields $l = 155 \text{ \AA}$. It therefore follows that the thickness of the polar-ordered layer can be $\sim 10^2 \text{ \AA}$, which is close to the estimate $l = 60\text{--}70 \text{ \AA}$ deduced from the expression $l = 2D_{\parallel}\tau_{\parallel}$ obtained in Ref. 4; here, D_{\parallel} is the diffusion coefficient along the director.

The polar order was observed in Ref. 13 for a monolayer of octylcyanobiphenyl at the interface between liquid crystal phase and glass in experiments involving second harmonic generation. The surface polarization reported in Ref. 13 was independent of temperature, which was to be expected for a monolayer.

In the other limiting case, when the thickness of a sample is $h \gg l \approx 100 \text{ \AA}$ (for example, if $h \approx 4\text{--}20 \text{ \mu m}$, as in Ref. 14) the surface polarization is in principle detectable, but its temperature dependence is not manifested experimentally since when heating reduces l even severalfold, the changes are still negligible compared with the macroscopic thickness of the sample. This is possibly the reason for the absence of the temperature dependence of the surface polarization reported in Ref. 14 and for the absence of the dependence $\tau_1(T)$ in the case of macropores. In fact, even for a typical macropore size $R_2 = 1000 \text{ \AA}$, we have $l < R_2$ and the temperature dependences of the effects due to the surface polar order can be detected provided we use objects with the characteristic size $\sim l$, which occurs in micropores. This circumstance was manifested particularly clearly in the case of CPHB.

4. ACS AND CPHB IN MICROPORES AND MACROPORES

1. *The $\epsilon = \epsilon(T)$ dependence.* Figure 7 shows the temperature dependence of $\langle\epsilon\rangle$ for CPHB in micropores (curve 1) and in macropores (curve 2). Typical dependences $\epsilon(T)$ obtained for ACS are given in this figure for the case of ACS-1

in micropores (curve 3) and ACS-2 in macropores (curve 4). Curves 1 and 3 (micropores) show no singularities typical of a transition to the isotropic phase. In the case of CPHB (curve 1) at $T > 350 \text{ K}$, when the liquid crystal in the free state is isotropic, a steep rise of ϵ is observed, as in the case of substances with the spontaneous polarization as T approaches the critical point. We shall show below that the rise of ϵ is accompanied by critical slowing down of relaxation. In the case of ACS the quasistatic values of ϵ was not reached at the frequencies employed and, in contrast to CPHB, the rise of ϵ at $T > 305 \text{ K}$ could not be interpreted unambiguously.

Transitions to the solid phase in micropores were observed at the following temperatures: $T_{CN}^{(R)} \approx 257 \text{ K}$ (CPHB), $T_{CN}^{(R)} \approx 252 \text{ K}$ (ACS-1), and $T_{CN}^{(R)} \approx 255 \text{ K}$ (ACS-2). In the case of CPHB in macropores there were two transitions (curve 2). At $T < 313 \text{ K}$ it was found that the behavior was typical of solids and that $\epsilon \rightarrow n^2$, corresponding to freezing of the dipole contribution to the polarization. A similar behavior was also observed for ACS-2 (curve 4) and the temperature $T \approx 306 \text{ K}$ could be attributed to the transition to the solid phase, but dielectric measurements showed no transition to the isotropic phase for ACS in macropores and micropores. In the case of CBHP the temperature $T = 332 \text{ K}$ on curve 2 could be attributed to the transition to the isotropic phase, i.e., T_{NI} increased compared with the free state. The shifts of T_{CN} and T_{NI} are discussed in Sec. 6 together with the data on 5CB.

2. *The $\epsilon = \epsilon(\nu)$ dependence.* Figure 8 shows the dispersion curves obtained for ACS-1 at various temperatures. Clearly, the quasistatic value ϵ_s was not reached so that τ_1 gave ambiguous results and the first dispersion region appeared at $\nu \sim 10^3 \text{ Hz}$, which could be due to the Maxwell-Wagner polarization mechanism, and it was not possible to suggest an interpretation of $\epsilon(\nu)$ in the range $\nu < 10^5 \text{ Hz}$ in a reasoned manner.

The dependence of τ_2 on T^{-1} is plotted for ACS-1 in Fig. 6 (line 7c). The results of measurements of ϵ' and ϵ'' for CPHB are plotted in Fig. 9a. The inset shows the results of direct measurements of ϵ'_c as a function of temperature and

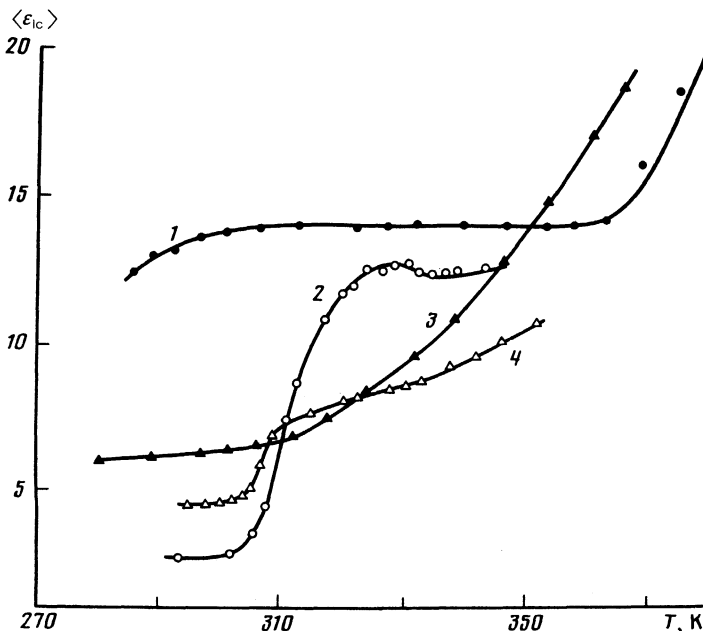


FIG. 7. Temperature dependences of the permittivity: 1) CPHB in micropores at 1 kHz; 2) CPHB in macropores at 1 kHz; 3) ACS-1 in micropores at 10 kHz; 4) ACS-2 in macropores at 10 kHz.

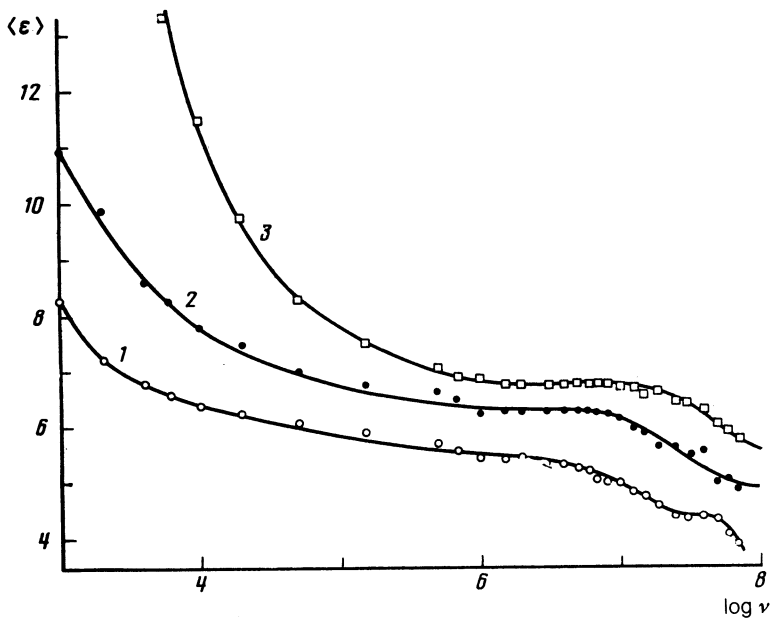


FIG. 8. Frequency dependences of the permittivity of ACS-1 in micropores at various temperatures: 1) $T = 297$ K; 2) 318 K; 3) 341 K.

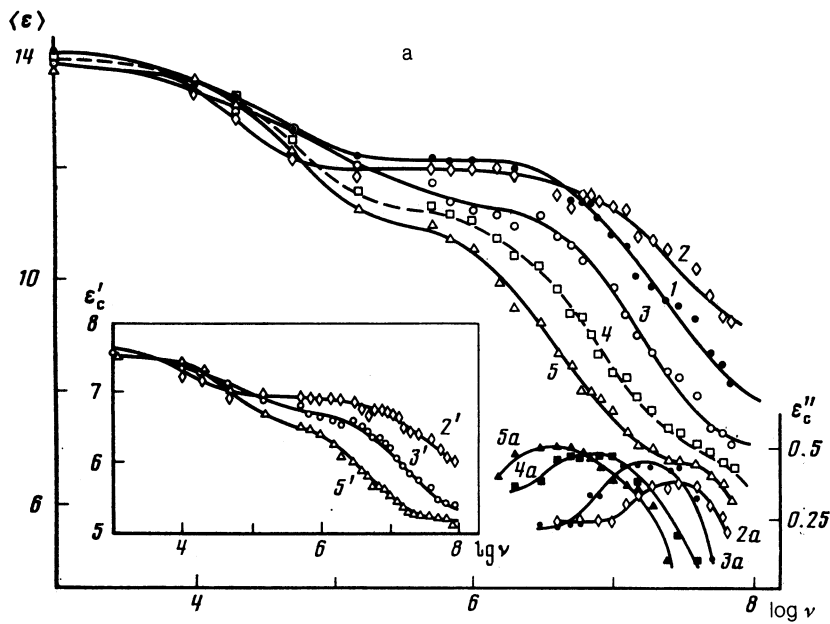
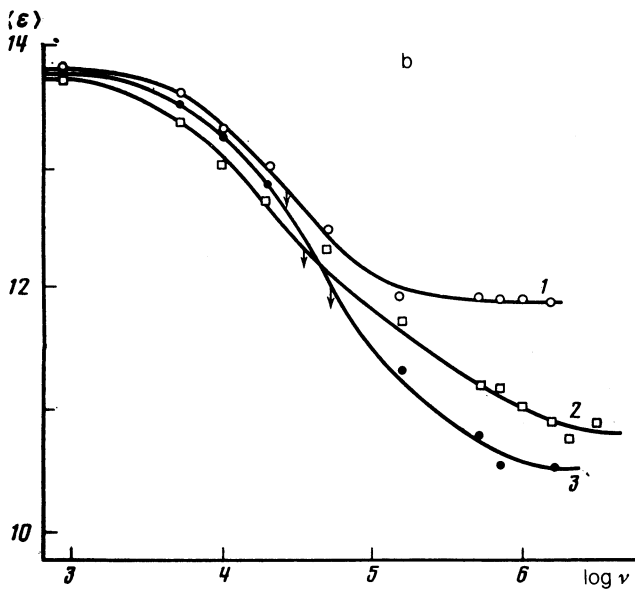


FIG. 9. a) Frequency dependences of the permittivity and of the dielectric loss factor of CPHB in micropores at various temperatures: 1) $T = 363$ K; 2) 383 K; 3) 343 K; 4) 328 K; 5) 318.5 K; all these five curves represent $\langle \epsilon \rangle$; 2a), 3a), 4a), 5a), ϵ''_c . The inset shows ϵ'_c . b) Frequency dependence of the permittivity in the first dispersion region at different temperatures: 1) $T = 363$ K; 2) 343 K; 3) 318.5 K. The vertical arrows identify the frequencies corresponding to τ_1 .



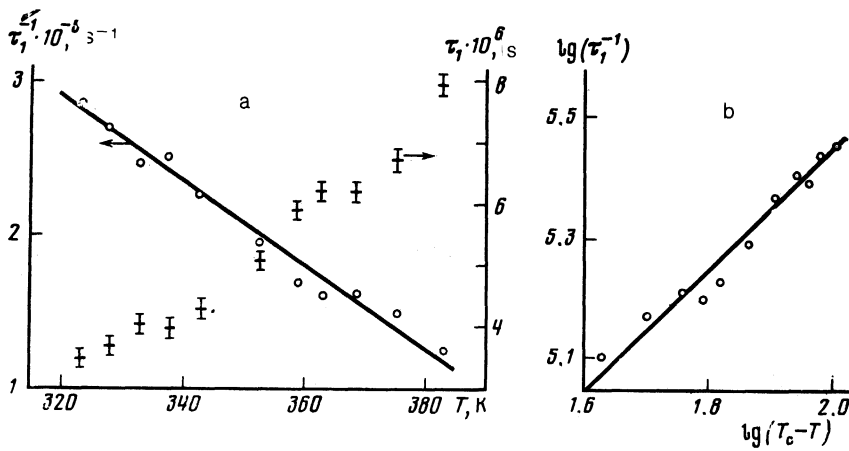


FIG. 10. a) Temperature dependences of the relaxation time τ_1 and of its reciprocal τ_1^{-1} for CPHB in micropores. b) Dependence of $\log(\tau_1^{-1})$ on $\log(T_c - T)$ for CPHB in micropores.

the corresponding Cole–Cole diagrams are shown in Fig. 5 (curves 3, 4, and 5). The Cole–Cole parameters corresponding to these curves have the values $\alpha_3 = 0.1$ ($T = 318.5$ K), $\alpha_4 = 0.14$ ($T = 343$ K), $\alpha_5 = 0.17$ ($T = 383$ K), i.e., there is a common relationship: the relaxation times have a spectrum in the second dispersion region. In the free state the Cole–Cole parameter for τ of CPHB is zero.²⁵ The temperature dependence of τ_2 splits into two regions and at $T < 345$ K it is represented by line 5b, whereas at $T > 345$ K it is represented by line 6b. It therefore follows that at temperatures $T > 350$ K there is not only the quasistatic growth of $\langle \epsilon \rangle$ but also a change in the dynamics of orientational motion of the molecules responsible for the second dispersion region. The $\tau_2(T)$ dependence for CPHB is weaker, as in all the other investigated cases, than the $\tau_{||}(T)$ dependence in the free state.

The ratio of the If increment $\Delta\epsilon_3$ (Fig. 3) to $\Delta\epsilon_1$ is 1.65. On the other hand, we know that $(\Delta\epsilon_3/\Delta\epsilon_1) \approx \mu_3^2/\mu_1^2 = 1.5$, which is in good agreement with the experimental value. An estimate of the thickness of the polar-ordered layer in CPHB gives $l \approx 120$ Å.

3. Soft mode and critical reduction in τ_1 for CPHB in micropores. Figure 9a shows that the dispersion curves corresponding to the first region, which is associated with the surface polar order, are shifted toward lower frequencies on increase in T . This is illustrated clearly in Fig. 9b, where typical dependences $\epsilon''(\nu)$ are plotted for the first dispersion region and the vertical arrows identify the frequencies corresponding to τ_1 . The dependence of τ_1 on T is presented in Fig. 10 and the experimental points exhibit a trend typical of the critical relaxation retardation describing the soft mode in ferroelectric liquid crystals.²⁶ As is known,²⁶ in the case of the C smectics a soft mode may be in the form of in-phase fluctuations of the amplitude of the angle of tilt of the molecules (between the axis of a molecule and the normal to the smectic layer) and of the polarization, which are order parameters. In the case of CPHB the nature of the polar contribution is quite different in micropores, but one of the order parameters can be the angle θ between the dipole and the normal to the surface of a pore.

The molecules of CPHB have, unlike those investigated earlier, a large dipole moment. This has the effect that the dimensionless parameter $n\mu^2/k_B T$ (n is the number of molecules in 1 cm^3 and k_B is the Boltzmann constant), representing the ratio of the energy of the dipole–dipole interaction to the energy of thermal motion, is 1.4, whereas even in the case

of 5CB it is found that $n\mu^2/k_B T = 0.94$. The electrostatic interaction of dipole molecules in liquid crystals is insufficient to overcome the disordering effect of the thermal motion and creation of a polar order, but near the solid surface of pores the polarization state is dependent on at least two factors: a very strong dipole–dipole (static) interaction and the interaction with the wall of a pore, which stabilizes the orientational order and suppresses the thermal fluctuations. The curvature of the surface of a pore may be another important factor in the establishment of a polar order.

Thus, if we select the order parameter in the form of the angle θ , we can use the familiar expression for τ , which describes a soft mode due to relaxation of the molecular tilt angle²⁶:

$$\tau = \gamma_1 / 4a'(T_c - T), \quad T < T_c, \quad (5)$$

where in the case of pores we have the effective viscosity γ_1 and the coefficient a' is in front of the quadratic term in the expansion of the free energy in powers of the order parameter. The critical exponent in Eq. (5) is unity (mean-field theory).

It is clear from Fig. 10a that the dependence of the reciprocal of the relaxation time τ_1^{-1} on T is linear. Extrapolation to the value $\tau_1^{-1} = 0$ makes it possible to determine the amplitude $T_c = 426.5$ K which in this case can be regarded as a fitting parameter, which is of considerable importance to the critical temperature. Measurements at temperatures closer to T_c than those used by us are impossible because further heating results in a thermal oxidation and destruction of the investigated material. Figure 10b shows the dependence of $\log(\tau_1^{-1})$ on $\log(T_c - T)$ showing clearly that the relevant critical exponent should be 1 ± 0.15 and $a'/\gamma_1 = 800 \text{ s}^{-1} \cdot \text{K}^{-1}$. Assuming²⁶ that $a' \approx 10^3 \text{ erg} \cdot \text{cm}^{-3} \cdot \text{K}^{-1}$, we estimate γ_1 to have the value $\gamma_1 \approx 1.25 \text{ P}$, which is a reasonable value for the viscosity coefficient.

5. $\tau_2(T)$ DEPENDENCE AND SURFACE ENERGY OF NEMATIC LIQUID CRYSTALS

It is clear from Fig. 6 that the dependence of $\ln\tau_2$ on T^{-1} was linear for all the investigated crystals. It follows that the dependence $\tau_2(T)$ can be described by the linear relationship

$$\tau = \tau_0 \exp(U/k_B T),$$

where U is the activation energy which in the barrier theories

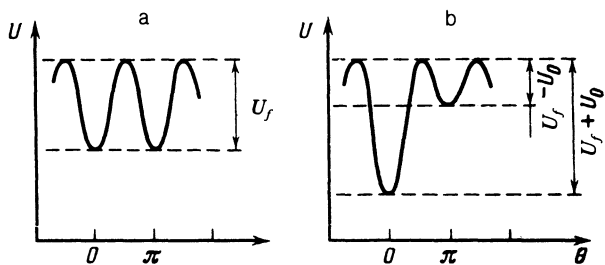


FIG. 11. Dependence of the potential on the angle θ : a) nematic liquid crystal in the free state; b) nematic liquid crystal in pores.

is equal to the difference between the potential energy of one of the stable orientations $\theta = 0$ or π (θ is the angle between the director and the dipole) and the highest potential energy of intermediate orientation ($\theta = \pi/2$). There is no polar order in the free state and, therefore, the orientations $\theta = 0$ and $\theta = \pi$ are equiprobable (Fig. 11, curve a). The values of the activation energies of the investigated nematic liquid crystals in the free state were found to be $U_{1f} = 8.8 \times 10^{-13}$ erg for 5CB; $U_{2f} = 8.3 \times 10^{-13}$ erg for ACS-1, and $U_{3f} = 14 \times 10^{-13}$ erg for CPHB.

The interaction of nematic liquid crystal molecules with the surface (characterized by the interaction energy U_0) is equivalent to the interaction with an external field which ensures a polar order near the surface and this polar order stabilizes one orientation ($\theta = 0$) and the corresponding change of U_f to $U_f + U_0$. If $\theta = \pi$, the potential becomes $U = U_f - U_0$ (curve b in Fig. 11) and it represents the activation energy. The potential energy for the $\theta = \pi/2$ orientation does not change in the linear approximation.

The activation energies U_i corresponding to the dependences $\tau_2(T^{-1})$ in micropores were found to be as follows: $U_1 = 1.7 \times 10^{-13}$ erg for 5CB, $U_2 = 4.9 \times 10^{-13}$ erg for ACS-1, and $u_3 = 8.5 \times 10^{-13}$ erg for CPHB at $T < 345$ K. The changes in the activation energy observed for CPHB in the range $T > 345$ K (line 6b in Fig. 6) was primarily due to a reduction in U_f . A comparison of U_f and U_i gave the energy of the interaction of molecules with the surfaces of the pores $U_{oi} = U_f - U_i$ and these values were $U_{o1} = 7.1 \times 10^{-13}$ erg, $U_{o2} = 3.4 \times 10^{-13}$ erg, and $U_{o3} = 5.5 \times 10^{-13}$ erg. Bearing in mind that these estimates were only qualitative, it would be reasonable to assume that $U_0 \approx 5 \times 10^{-13}$ erg.

The value of U_0 for macropores (line 4a in Fig. 6) was less than U_{o1} and amounted to $U_0 = 1.3 \times 10^{-13}$ erg. This was due to the fact that not all the molecules exhibited surface behavior and an estimate based on Eq. (4) indicated that only the fraction of molecules located in a layer of thickness $l \approx 100$ Å exhibited such behavior. Allowing for the bulk fraction of the molecules $g = 0.285$ in the surface layer

with polar ordering, we estimated U_0 to be 4.6×10^{-13} erg, in agreement with the above estimate.

Bearing in mind that the number of molecules of the investigated substances was $n_s \approx (2-3) \times 10^{14}$ cm $^{-2}$, we found that the surface energy of the nematic liquid crystal $F_0 = U_0 n_s$ should be $F_0 \sim 10^2$ erg/cm 2 . This value was in agreement with the estimate of Ref. 4, where $F_0 \sim \rho c^2 a \sim 10^2$ erg/cm 2 was obtained; here, the density ρ of the nematic liquid crystal, the velocity of sound in this liquid crystal c , and is the molecular size a are all typical of nematics.

6. SHIFTS OF T_{CN} AND T_{NI} REGARDED AS THE SIZE EFFECT AND THE RESULTS OF INTERACTION OF MOLECULES WITH THE SUBSTRATE

A reduction in the temperature of the appearance of a solid phase in the pores, irrespective of whether melting of a liquid crystal occurs or whether it forms an isotropic phase, has been established for a large number of samples in different matrices.¹⁰ Melting in pores does not differ fundamentally from melting of free particles in a strongly disperse state and in both cases the process can be regarded as the size effect (we are talking here of the size of the particles which melt and not the dimensions of space). The presence of a curved pore surface may only facilitate breakdown of the long-range positional order and in the limiting case of a monolayer it can result in complete absence of such order. The shift of the melting point $\Delta T_{CN} = T_{CN} - T_{CN}^{(R)}$ is described by the Thomson expression:

$$\Delta T_{CN} = 2T_{CN}\sigma_{CN}/q_{CN}\rho_c R, \quad (6)$$

where q_{CN} is the heat of melting per gram of substance; in the case of the investigated nematic liquid crystals we found that $q_{CN} \approx 50 \times 10^7$ erg/g, $\rho_c \approx 1$ g/cm 3 , and σ_{CN} is the interface (crystal-liquid crystal) surface energy. Determination of the melting point of the substance in the pores is a task which is relatively simpler to carry out experimentally than corresponding investigations of free tiny particles, because the size of the pores is fixed and known in advance. All the quantities in Eq. (6) were determined from independent experiments, with the exception of σ_{CN} , so that measurement of the shift in the pores can be regarded as an experimental method for the determination of σ_{CN} , which would be of interest on its own. The values of σ_{CN} determined for the first time for the investigated substances are listed in Table I and are close to the value of σ_{CL} (for the crystal-liquid transition) in the case of organic substances, for example, in the case of naphthalene it is known¹⁰ that $\sigma_{CL} = 30$ erg/cm 2 .

The size effect applies also to the transition from the

TABLE I. Interphase (crystal-liquid crystal) surface energies σ_{CN} and energies W of adhesion of liquid crystals to substrates.

Liquid crystal	Macropores, $R = 1000$ Å		Micropores, $R = 65$ Å	
	σ_{CN} , erg/cm 2	W , erg/cm 2	σ_{CN} , erg/cm 2	W , erg/cm 2
5CB	51	0.8	45	0.85
CPHB	36	1.2	31	—
ACS-1	25	—	27	—
ACS-2	24	—	28	—

liquid state to the isotropic liquid, but in this case we have $\sigma_{NI} = \sigma_N - \sigma_I \sim 10^{-2}$ erg/cm², i.e., this quantity is three orders of magnitude less than σ_{CN} and the lowering of T_{NI} responsible for this effect does not exceed 10^{-1} K to the nearest order of magnitude. The observed rise of T_{NI} in the pores cannot be attributed to the size effect. The increase in T_{NI} can be explained qualitatively by the orienting influence of the surface on the field, thus stabilizing the orientational order. In a quantitative description of this effect we must allow for the contribution made to the bulk density of the free energy by the anisotropic part of the surface energy, which is due to the polar order and is given by⁴

$$F_{or} = -W(\mathbf{n}\mathbf{v}) \frac{S}{V}, \quad (7)$$

where \mathbf{v} is the normal to the surface, \mathbf{n} is the director, and W is the anisotropic part of the surface energy of the liquid-crystal phase (representing the energy of adhesion of a liquid crystal to its substrate), which vanishes for the isotropic phase.

The condition of equilibrium of the phases subject to Eq. (7) is of the form

$$F_{NV} + \sigma_N \frac{S}{V} - W(\mathbf{n}\mathbf{v}) \frac{S}{V} = F_{IV} + \sigma_I \frac{S}{V}, \quad (8)$$

where F_{NV} and F_{IV} are the bulk terms of the free energy in the nematic and isotropic phases, and σ_N and σ_I are the corresponding surface tension coefficients. Bearing in mind that $F_{IV} - F_{NV} = q_{NI}\rho(1 - T_{NI}^{(R)}/T_{NI})$ and $S/V = 2/R$ for a cylindrical pore and that $\sigma_{NI} = \sigma_N - \sigma_I$ and also assuming that under equilibrium conditions we have $\mathbf{n}\mathbf{v} = 1$ ensuring the minimum of F_{or} , we find that the shift of the temperature of the transition to the isotropic phase is

$$T_{NI}^{(R)} - T_{NI} = \frac{2T_{NI}}{q_{NI}\rho R} (W - \sigma_{NI}), \quad (9)$$

where q_{NI} is the heat of the transition from the nematic to the isotropic phase, which has the value 2×10^7 erg/g typical of nematic liquid crystals. The values of W calculated using Eq. (9) are listed in Table I and are close to 1 erg/cm².

7. CONCLUSIONS

Direct experiments showed that a surface polar-ordered layer of $\sim 10^2$ Å thickness is located near the interface between a nematic liquid crystal and glass. In the case of a strongly polar nematic liquid crystal in micropores it was found for the first time that there was a soft mode associated with the polar order and absent in nematic liquid crystals in the free state, the relaxation time for which it was found to depend critically on temperature and the critical exponent was predicted by the Landau theory.

The difference between the dynamics of orientational motion of nematic liquid crystals in pores appears at a distance of $\sim 10^2$ Å and it is qualitatively determined by the total energy of the interaction between molecules and the surface, amounting to $F_0 \approx 10^2$ erg/cm². The anisotropic part of this energy representing the energy of adhesion of a

nematic liquid crystal to the substrate, is responsible for the shift of the phase transition temperature from the nematic to the isotropic phase and it amounts to 1 erg/cm².

The authors are grateful to E. I. Kats, V. V. Lebedev, and M. A. Osipov for discussing the results, and to E. I. Ryumtsev and A. P. Kovshik for their encouragement.

¹J. G. Dash, Phys. Rev. B **25**, 508 (1982).

²M. Shimoda, T. Mizusaki, M. Hirai, A. Hirai, and K. Eguchi, J. Low Temp. Phys. **64**, 285 (1986).

³Y. Kondo, Y. Kodama, Y. Hirayoshi, and T. Mizusaki, A. Hirai, and K. Eguchi, Phys. Lett. A **123**, 471 (1987).

⁴L. M. Blinov, E. I. Kats, and A. A. Sonin, Usp. Fiz. Nauk **152**, 449 (1987) [Sov. Phys. Usp. **30**, 604 (1987)].

⁵K. Miyano, J. Chem. Phys. **71**, 4108 (1979); Phys. Rev. Lett. **43**, 51 (1979).

⁶L. M. Blinov and A. Yu. Kabaenkov, Zh. Eksp. Teor. Fiz. **93**, 1757 (1987) [Sov. Phys. JETP **66**, 1002 (1987)].

⁷P. Sheng, Phys. Rev. Lett. **37**, 1059 (1976); Phys. Rev. A **26**, 1610 (1982).

⁸Y. Iimura, H. Mada, and S. Kobayashi, Phys. Lett. A **103**, 342 (1984).

⁹F. M. Aliev and M. N. Breganov, Pis'ma Zh. Eksp. Teor. Fiz. **47**, 97 (1988) [JETP Lett. **47**, 117 (1988)].

¹⁰D. Armitage and F. P. Price, Chem. Phys. Lett. **44**, 305 (1976); J. Polym. Sci. Polym. Symp. **63**, 95 (1977); Mol. Cryst. Liq. Cryst. **44**, 33 (1978).

¹¹M. V. Kurik, Fiz. Tverd. Tela (Leningrad) **19**, 1849 (1977) [Sov. Phys. Solid State **19**, 1081 (1977)].

¹²M. Kuzma and M. M. Labeš, Mol. Cryst. Liq. Cryst. **100**, 103 (1983).

¹³P. Guyot-Sionnest, H. Hsiung, and Y. R. Shen, Phys. Rev. Lett. **57**, 2963 (1986).

¹⁴L. A. Beresnev, L. M. Blinov, S. A. Davidyan, S. G. Kononov, and S. B. Yablonskii, Pis'ma Zh. Eksp. Teor. Fiz. **45**, 592 (1987) [JETP Lett. **45**, 755 (1987)].

¹⁵G. Barbero, I. Dozov, J. F. Palierne, and G. Durand, Phys. Rev. Lett. **56**, 2056 (1986).

¹⁶B. R. Ratna and R. Shashidhar, Mol. Cryst. Liq. Cryst. **42**, 1195 (1977); P. G. Cummins, D. A. Dunmur, and D. A. Laidler, Mol. Cryst. Liq. Cryst. **30**, 109 (1975).

¹⁷V. N. Tsvetkov, A. P. Kovshik, E. I. Ryumtsev, et al., Dokl. Akad. Nauk SSSR **222**, 1393 (1975).

¹⁸E. I. Ryumtsev, A. P. Kovshik, S. G. Polushin, and V. N. Tsvetkov, Kristallografiya **30**, 131 (1985) [Sov. Phys. Crystallogr. **30**, 73 (1985)].

¹⁹S. P. Zhdanov, *Physics and Chemistry of Silicates* (ed. by M. M. Shul'ts and R. G. L. Grebenshchikov) [in Russian], Nauka, Moscow (1987), p. 175.

²⁰F. M. Aliev and K. S. Pozhivilko, Fiz. Tverd. Tela (Leningrad) **30**, 2343 (1988) [Sov. Phys. Solid State **30**, 1351 (1988)].

²¹T. L. Chelidze, A. I. Derevyanko, and O. D. Kurilenko, *Electrical Spectroscopy of Heterogeneous Systems* [in Russian], Naukova Dumka, Kiev (1977).

²²F. M. Aliev, Pis'ma Zh. Eksp. Teor. Fiz. **41**, 254 (1985). [Sov. Phys. JETP **41**, 310 (1985)].

²³M. Massalska-Arodz, J. K. Mościcki, and S. Wróbel, Acta Phys. Pol. A **58**, 443 (1980).

²⁴C. Druon and J. M. Wacrenier, Mol. Cryst. Liq. Cryst. **88**, 99 (1982).

²⁵V. N. Tsvetkov, E. I. Ryumtsev, S. G. Polushin, and A. P. Kovshik, Dokl. Akad. Nauk SSSR **254**, 619 (1980) [Sov. Phys. Dokl. **25**, 753 (1980)].

²⁶L. M. Blinov and L. A. Beresnev, Usp. Fiz. Nauk **143**, 391 (1984) [Sov. Phys. Usp. **27**, 492 (1984)].

Translated by A. Tybulewicz